Lung Cancer 218 (2026) 109512

Contents lists available at ScienceDirect

Lung Cancer

journal homepage: www.elsevier.com/locate/lungcan

Research Paper

Genome-wide copy number analysis identifies AKT as a novel therapeutic target in pleural mesothelioma

Claudia Kalla [a,b,c,1,*], Dina Mönch [a,c,d,1], Sophia Steinlein [a,b,c], Alessandro Pastore [e], Heike Horn [a,b,c], Roger Falkenstern-Ge [f], Julia Schüler [g], German Ott [b], Gerhard Preissler [h]

[a] Dr. Margarete Fischer-Bosch Institute of Clinical Pharmacology, 70376 Stuttgart, Germany
[b] Department of Clinical Pathology, Robert Bosch Hospital 70376 Stuttgart, Germany
[c] Department of Clinical Pharmacology, University Hospital, University of Tübingen 72076 Tübingen, Germany
[d] German Cancer Consortium (DKTK), German Cancer Research Center (DKFZ), 72076 Tübingen, Germany
[e] Memorial Sloan Kettering Cancer Center, New York, NY 10065, USA
[f] Department of Molecular and Pneumonological Oncology, Robert-Bosch-Hospital, 70376 Stuttgart, Germany
[g] Charles River Laboratories Germany GmbH, 79108 Freiburg, Germany
[h] Department of Thoracic Surgery, RBK Lung Center, Robert Bosch Hospital, 70376 Stuttgart, Germany

ARTICLE INFO

Keywords:
Pleural mesothelioma
AKT
Ipatasertib
Sapanisertib
OncoScan CNV analysis

ABSTRACT

Purpose: Targeting aberrantly activated kinases in pleural mesothelioma (PM) is a promising therapeutic strategy. To identify potential candidates, we characterized recurrent chromosomal gains in PM and subsequently evaluated the specific inhibition of kinases that were activated by amplification and/or overexpression.
Methods: 42 primary PM were screened for chromosomal alterations using OncoScan technology and AKT expression was assessed using immunohistochemistry. The impact of Ipatasertib (pan-AKT inhibitor) and Sapanisertib (mTOR inhibitor) on cell survival, apoptosis induction, AKT/mTOR signaling, glycolysis was investigated in cell lines and primary cells. Preclinical anti-tumor efficacy was further assessed in a PDX model selected for AKT and mTOR expression.
Results: OncoScan profiling identified eleven regions of significant chromosomal gains. Among them, 14q32.33 and 19q13.2 gains affected AKT1 and AKT2, members of the AKT serine/threonine protein kinase family. AKT1 protein was expressed in 66 % (60/91), AKT2 in 80 % (73/91) and AKT3 in 94 % (86/91) PM. 57 % PM co-expressed AKT1/AKT2/AKT3. Treatment with Ipatasertib impaired cell viability in PM cell lines and induced apoptosis. Combined treatment with Ipatasertib and Sapanisertib had a synergistic cytotoxic effect in all three cell lines and primary cells from two PM patients, even in Cisplatin-resistant cells. We also noted an improved response to the combination in a PDX model. Mechanistically, the combined treatment acted synergistically to inactivate AKT/mTOR downstream signaling, suppress glycolysis, and trigger ATP depletion.
Conclusions: Our study demonstrates recurrent activation of AKT kinases by copy number gains and upregulated expression in PM. Pharmacological AKT and mTOR inhibition is a promising therapeutic alternative for mesothelioma.

1. Introduction

Pleural mesothelioma (PM) is an aggressive cancer originating from mesothelial cells of the pleura associated with poor prognosis. PM are classified into three major histologic subtypes – epithelioid, biphasic, and sarcomatoid. Regardless of the histological subtype, most PM are diagnosed in advanced stage and show multi-focal growth at the time of diagnosis, so that surgery combined with radio-chemotherapy benefits only a small subset of patients presenting with early-stage disease [1]. Cisplatin combined with pemetrexed or raltitrexed long served as standard treatment for advanced PM, with a median survival of about one year [2]. However, this regimen was effective in merely 25–30 % of

* Corresponding author at: Dr. Margarete Fischer-Bosch Institute of Clinical Pharmacology, Auerbachstr. 112, 70376 Stuttgart, Germany.
E-mail address: claudia.kalla@ikp-stuttgart.de (C. Kalla).
[1] These authors contributed equally to this study.

https://doi.org/10.1016/j.lungcan.2026.109512
Received 4 February 2026; Received in revised form 23 June 2026; Accepted 26 June 2026
Available online 28 June 2026

the patients [3,4]. Recent trials with immune checkpoint inhibitors nivolumab plus ipilimumab achieved an objective response rate of 40 % and superior overall survival compared to chemotherapy (18.1 vs. 14.1 months; HR, 0.74 [95 % CI, 0.62 to 0.88]) [5,6]. Based on these results, first-line combination immunotherapy has been established as the new standard of care [7]. Despite those significant improvements, there is still an unmet need for new therapeutic options, especially for non-responding patients. New drugs targeting aberrantly activated signaling molecules may be promising therapeutics in PM.

In contrast to other tumor entities, mesotheliomas show a rather limited number of genomic alterations and – therefore – shortage of druggable targets. The key genomic alterations implicated in PM pathogenesis are deletions and inactivating mutations of tumor suppressors *NF2*, *CDKN2A/B* and *BAP1* seen in about 40 %, 75 % and 25 % of PM, respectively [8–10]. These genes are involved in transmembrane and intracellular signaling, response to DNA damage, cell cycle control and cell proliferation. Consequently, disruption of their function promotes PM cell proliferation and metastasis. While direct restoration of NF2, CDKN2A/B and BAP1 function is not feasible, targeting of aberrantly activated downstream effectors to treat PM appeared as a promising strategy. Deletion of *NF2* leads to aberrant activation of the serine/threonine protein kinase mTOR that regulates protein, lipid and nucleotide synthesis, cell proliferation, survival, and autophagy [11,12]. Inhibition of mTOR by Rapamycin or its derivatives suppressed mesothelioma cell growth in preclinical models [11,13,14], but was not effective in clinical trials (NCT00770120, NCT01024946) [15].

Recent research has been directed towards identifying aberrantly activated kinases for targeted treatment of PM. Various studies have reported on the expression and activation of receptor tyrosine kinases in mesothelioma, including EGFR, MET, IGFR, FGFR1, and VEGFR [16–18]. Specific inhibition of VEGFR, FGFR1, MET or EGFR suppressed mesothelioma cell growth *in vitro* [16–21]. However, clinical studies with kinase inhibitors as single agents yielded only disappointing results. VEGFR inhibition, e.g. had minimal activity in PM and was poorly tolerated [22,23], and EGFR or MET inhibition was clinically ineffective in PM patients, despite high expression of EGFR (NCT00025207, NCT00039182) [24,25] and MET (NCT01861301). The poor response of VEGFR-, EGFR- or MET-targeted therapies raises the question of whether those kinases represent key drivers in the genesis of PM. Therefore, we applied a whole-genome approach using the OncoScan Array to examine DNA copy number alterations and identify chromosomal regions that may harbor oncogenic drivers suitable for targeted treatment of mesothelioma cells. This approach allowed us to identify the AKT kinase as an aberrantly activated oncogene with relevant therapeutic implications in the majority of mesotheliomas. Through comprehensive preclinical investigations, this study substantially advances previous findings regarding AKT1 and AKT3 expression in PM cell lines, and the expression of phosphorylated AKT in 65–88 % patients [26–28]. Additionally, our data confirm the cytotoxic efficacy of specific AKT inhibition in PM cells [29,30] and highlight simultaneous AKT/mTOR inhibition as a promising therapeutic strategy.

2. Materials and methods

2.1. Tumor specimens

Formalin-fixed paraffin-embedded (FFPE) resection specimens from 99 PM patients were analyzed within this study, including 10 sarcomatoid, 69 epithelioid and 20 biphasic PM. Histological diagnoses, reviewed independently by experienced pathologists (G.O., Sabine Bode-Erdmann), were formulated according to the 2015 WHO Classification. Patients were enrolled at Robert Bosch Hospital Stuttgart (Germany) between 2001 and 2013 and received chemotherapy with either cisplatin or cisplatin/pemetrexed; treatment data were unavailable for 49 patients. All tumor samples were collected prior to treatment. Clinical data were retrieved from institutional medical records. Lymph node metastases were confirmed via surgical resection. Distant organ metastases (longest diameter $\geq$ 10 mm) were monitored via contrast-enhanced CT (5–7 mm slice thickness) and FDG-PET/CT using standard RECIST 1.0, and pleural manifestations using 2004 modified RECIST (thickness $\geq$ 10 mm). Triplicate 0.6 mm tumor cores were inserted into tissue microarrays (TMA) used for all immunohistochemistry (IHC) analyses. All investigations were conducted in accordance with ethical standards and in compliance to the Helsinki Declaration and national and international guidelines. They were approved by the Ethics Committee of the University Hospital, Tübingen, Germany (344/2012BO2).

2.2. Cell lines

Mesothelial cell line Met-5A was purchased from American Cell Culture Collection (ATCC CRL-9444). PM patient-derived xenograft (PDX) cell lines PXF698, PXF1118 (both epithelioid PM) and PXF1752 (sarcomatoid PM) were provided by Charles River Laboratories Germany (Freiburg, Germany). The cell lines had been derived from the respective PDX tumors and cultured in RPMI medium with 10 % FBS (Merck, Darmstadt, Germany). Primary PM-cell lines MPM186 and MPM187 were established from PM tissues (both epithelioid PM) obtained from two chemo-naïve patients who had undergone surgical procedure at the Robert Bosch Hospital (Stuttgart, Germany). Fresh tumor tissue was minced into pieces < 1 mm^3 and digested using the Tumor Dissociation Kit (human) with the gentleMACS Octo Dissociator (Miltenyi Biotec, Bergisch-Gladbach, Germany) for 1 h at 37 °C. Following short centrifugation at 40xg, cells were collected from the supernatant by centrifugation at 300xg for 5 min and cultured in Advanced DMEM/F12 medium (ThermoFisher Scientific, Waltham, MA, USA) with 10 % FBS Superior (Merck), 1 % penicillin–streptomycin (ThermoFisher Scientific), 1 % L-glutamine (Bio&Sell, Feucht, Germany), 50 ng/ml hEGF (ThermoFisher Scientific), 10 μM Y-27632 (Selleckchem, Houston, TX, USA). The PM origin of cells was confirmed by immunostaining of cells fixed in 4 % formalin with antibodies against calretinin, WT1 and BAP1, in comparison with FFPE tissue of the same tumor. Normal fibroblasts were gained from reactive lymph node resections as described previously and cultured in RPMI supplemented with 20 % FBS [31].

2.3. Antibodies and reagents

Antibodies to detect PARP1 (46D11), AKT1 (D9R8K), pan-AKT (C67E7), mTOR (7C10), p-AKT (Ser473, D9E), p-AKT (Ser473, 587F11), RPS6 (5G10), p-RPS6 (Ser235/236), PRAS40 (D23C7), p-PRAS40 (Thr246), GSK3b (D5C5Z), p-GSK3b (Ser9), p-ERK1/2 (Thr202/Tyr204, D13.14.4E), PTEN (138G6) were from Cell Signaling (Danvers, MA, USA). Anti-AKT2, Anti-AKT3, Anti-RPS6 (1C3E19) were purchased from Origene (Rockville, MD, USA), Abcam (Cambridge, UK) and ThermoFisher Scientific, respectively. Anti-β-Actin (AC-15), anti-calretinin (Cell Marque), anti-WT1 (6F-H2, Cell Marque) were from Sigma-Aldrich (München, Germany). Anti-BAP1 (C-4) was from Santa Cruz Biotechnology (Dallas, TX, USA). Ipatasertib, Sapanisertib (INK128), Paclitaxel were purchased from Selleckchem, Cisplatin from Merck.

2.4. Copy number microarray analysis

PM specimens were selected based on tumor cell content exceeding 50 %, and all sarcomatoid PM cases in our cohort meeting this criterion were included. Genomic DNA was purified from FFPE tumor tissues using the QIAamp FFPE Tissue Kit (Qiagen, Hilden, Germany) and quantified using the Qubit 2.0 fluorometer (ThermoFisher Scientific). Copy number variation analysis was performed with 80 ng genomic DNA using the OncoScan CNV Assay (ThermoFisher Scientific) for FFPE samples according to the manufacturer's instructions. The arrays were

hybridized in a GeneChip Hybridization Oven645 and scanned using the GeneChip3000 scanner (ThermoFisher Scientific). CEL files (GeneChip Command Console software output) generated from the scanned array image were normalized and centered using the apt-copynumber-oncoscan protocol (Affymetrix) and default settings. Reference files for the OncoScan copy number variation array were downloaded from the ThermoFisher Scientific website (NetAffxGenomicAnnotations. Homo_sapiens.hg19). CEL data were translated into log2 copy ratio data using the Expectation Maximization Algorithm [32]. Arm level events and focal events were called from segmented log2 copy ratio data using Genomic Identification of Significant Targets in Cancer (GISTIC2.0) [33] and the default settings except for ~ conf. 0.99, ~brlen 0.7, ~broad 1, ~armpeel 1. Samples were confirmed to have a robust CNV profile and a 9p22 (CDKN2A/B) status consistent with that examined by fluorescent in situ hybridization (ZytoLight SPEC CDKN2A/CEN9 Dual Color Probe, Zytovision, Bremerhafen, Deutschland) as described earlier [34]. The CNV data have been deposited at the European Genome-PhenomeArchive (EGA) and are accessible through accession number EGAS00001008478.

2.5. Immunohistochemistry

IHC was performed on 3-μM TMA sections and sections of FFPE-embedded cell lines using conventional DAB staining on a semi-automated autostainer (LabVision 720, Thermo Fisher Scientific). Non-tumor tissues (lymphnode, intestine, stomach) were used as on-slide controls. After heat-induced epitope retrieval, anti-AKT1 (1:200), anti-AKT2 (1:200), anti-AKT3 (1:300), pan-AKT (1:300), PTEN (1:200) or anti-mTOR (1:100) was incubated for 30 min. AKT and mTOR protein expression was assessed by combining the intensity of cytoplasmic staining (0, no staining; 1+, faint; 2+, moderate; 3+, strong) and the proportion of positive cells (1=<20 %; 2 = 20–50 %; 3 = 51–80 %; 4=>80 %). Staining results were evaluated in four grades according to the product of staining intensity and the percentage of positive cells: 0–1, negative; 2–3, weak; 4–8, moderate; 9–12 strong staining; moderate and strong staining were regarded as upregulated AKT protein expression (AKT^{high}), negative and weak staining were classified as AKT^{low}. PTEN deficiency was definied as staining in less than 10 % of tumor cells, regardless of intensity [35].

2.6. Cell viability assays

Cytotoxicity in PDX-cell lines was examined using the MTT assay. Cells ($4x10^3$ cells/100 μl) were seeded into 96-well plates and incubated with Ipatasertib, Sapanisertib or their combinations for 72 h. After addition of 5 mg/ml MTT reagent, cells were incubated for 2 h at 37 °C. The optical density of MTT was measured at 550 nm using the VICTOR Nivo microplate reader (PerkinElmer, Waltham, MA, USA). Percent viability was calculated by normalizing absorbance values to the values from cells grown in media without drug after background subtraction. In primary PM-cells, cytotoxicity was investigated using the CellTiter-Glo 2.0 assay (Promega, Madison, WI, USA) according to the manufacturer's protocol. Cells ($3x10^3$ cells/50 μl) were seeded into 96-well plates and incubated with 50 μl Ipatasertib, Sapanisertib or their combinations for 72 h. After addition of CellTiter-Glo reagent at a 1:1 ratio, plates were incubated for 10 min at room temperature. Luminescence was measured using the VICTOR Nivo microplate reader. Percent viability was calculated by normalizing luminescence values to those from cells grown in media without drug after background subtraction.

2.7. Cell death

For real-time investigation of apoptosis and necrosis, cells ($1x10^4$ cells/50 μl) were seeded into 96-well plates and incubated for 24 h at 37 °C. Ipatasertib (10 μM), Paclitaxel (400 nM) or DMSO (0.01 %) were added followed by immediate addition of Real Time-Glo Annexin V Apoptosis and Necrosis reagent (part# JA1011, Promega). Luminescence and fluorescence signals were monitored overtime up to 48 h using the VICTOR Nivo microplate reader (PerkinElmer).

2.8. Immunoblotting

Snap-frozen cells were homogenized in lysis buffer (50 mM TRIS-HCl pH 7.6, 250 mM NaCl, 5 mM EDTA, 0,1 % Triton X-100) containing cOmplete protease inhibitor cocktail and PhosSTOP phosphatase inhibitor (Roche, Mannheim, Germany) by zonication. Immunoblotting was performed as previously described [36]. Antibodies were used at 1:1.000 dilution, except antibodies against phospho-AKT (1:2.000), phospho-RPS6 (1:2.000), β-Actin (1:10.000). Luminescent signals were detected with the Stella3200 system (Raytest, Straubenhardt, Germany).

2.9. Bioluminescent cellular immunoassay

In primary PM-cells, p-AKT and p-S6RP levels were examined by using the Lumit Immunoassay Cellular Systems (Promega) according to the manufacturer's protocol. Cells ($5x10^4$ cells/50 μl) were seeded into 96-well plates and incubated with 10 μM Ipatasertib, 30 nM Sapanisertib or their combination for 8 or 24 h. Cells were lysed using Lysis Buffer II and vigorous mixing for 20 min. Then, 50 μl of an antibody mix containing two primary antibodies against p-AKT (Ser473, 587F11) and AKT (C67E7) or against p-S6RP (Ser235/236) and S6RP (1C3E19) and NanoBit detecting antibodies were added to the lysates. The plates were incubated for 90 min at room temperature, followed by the addition of Nano-Glo Luciferase Substrate. Luminescence was measured using the VICTOR Nivo microplate reader.

2.10. Assessment of ATP and lactate levels

ATP levels (CellTiter-Glo 2.0 assay; Promega) and lactate levels (Lactate-Glo assay; Promega) were analyzed in parallel according to the manufacturer's protocols. Cells (ATP: $3x10^3$ cells/50 μl, Lactate: $15x10^3$ cells/50 μl) were seeded into two 96-well plates and incubated with 50 μl 10 μM Ipatasertib, 30 nM Sapanisertib or their combination for 24 h. ATP levels were determined by addition of CellTiter-Glo reagent at a 1:1 ratio to plate 1, followed by luminescence measurement using the VICTOR Nivo microplate reader. For measuring lactate secretion, 4 μl of medium was removed from each sample of plate 2 and diluted 50-fold with PBS. A portion of each sample was mixed with Lactate-Glo reagent at a 1:1 ratio, incubated for 60 min at room temperature, followed by luminescence measurement. Percent ATP and lactate levels were calculated by normalizing luminescence values to those from cells grown in media without drug.

2.11. In vivo therapy study

The *in vivo* effect of Ipatasertib and Sapanisertib was examined using the PM patient-derived xenograft model PXF1752 established by Charles River Laboratories Germany GmbH (Freiburg, Germany). Tumor cells were implanted subcutaneously in NMRI nu/nu mice. Tumor-bearing mice with tumors 50–200 mm^3 in size were randomized into different treatment groups (n = 5/group): Vehicle control (orally), Ipatasertib (40 mg/kg/d, orally), Sapanisertib (0.3 mg/kg/d, orally), or combination treatment with Ipatasertib (40 mg/kg/d, orally) and Sapanisertib (0.3 mg/kg/d, orally). The length (L) and width (W) of each tumor was measured with calipers, and the body weight was determined every 3 to 4 days. Tumor volumes were $TV = L*W^{2}*0.5$; relative tumor volumes of individual tumors were $RTV = TV_{21}/TV_0*100$. All animal treatment procedures were conducted according to the guidelines of the German Animal Welfare Act and were approved by the Regional Administrative Authority of Freiburg (G-20/163).

2.12. Statistical analysis

Statistical tests were done using GraphPad Prism 5.0 and Analyse-it for Excel. The test used, the number of samples and the significance are indicated in the text and in the respective figure legends. P-values of < 0.05 were considered statistically significant. Survival data were analyzed using the Kaplan-Meier method combined with the Gehan-Breslow-Wilcoxon test (Bonferroni correction for multiple comparisons). The analyses were adjusted for identical therapy regimen (Cisplatin/Pemetrexed) but not for age or gender. The CompuSyn software was used for generating a combination index (CI) of drug combinations [37].

3. Results

3.1. Genomic gains in PM affect AKT genes

In order to identify copy number variations, we performed whole-genome copy number analyses using the OncoScan CNV Assay. The study included 42 primary PM specimens – nine sarcomatoid and 33 epithelioid – selected based on tumor cell content exceeding 50 % and an FFPE specimen age under 15 years. This ensured high-quality data by minimizing DNA degradation and maintaining optimal tumor-to-non-tumor ratios. GISTIC2.0 analysis revealed 15 significant deletion and eleven significant gain events (Fig. 1A, B, Table 1). Commonly deleted loci included those containing tumor suppressors *CDKN2A/B* on 9p21.3 (60 %), *NF2* on 22q (74 %), *BAP1* on 3p21.3 (31 %), and *TP53* on 17p13 (31 %). Significant copy number gains encompassed the loci of oncogenic drivers *MYC* on 8q24.2 (24 %), *JUND* (proto-oncogenic transcription factor) on 19p13.1 (10 %), *MKNK2* (MAPK interacting serine/threonine kinase 2) on 19p13.3 (57 %), *RAB21* (Ras oncogene family) on 12q21.1 (24 %), and *PIK3CA* (catalytic subunit alpha of PI3K) on 3q (19 %) (Table 1).

Furthermore, 14q32.33 and 19q13.2 gains affected *AKT1* and *AKT2*, two members of the AKT serine/threonine protein kinase family: 45 % (19/42) PM had three or four *AKT1* copies, 10 % (4/42) PM had four copies or an amplification of *AKT2*. On top of that, 19 % (8/42) PM had extra-copies of *AKT3* (1q43), the gene coding for the third AKT isoform, finally resulting in information on *AKT* gains in 66 % (28/42) PM (Fig. 1B, Suppl. Fig. 1, Suppl. Table 1). Gain events of the individual AKT genes were not mutually exclusive, so that three tumors had simultaneous *AKT1/AKT2*, *AKT1/AKT3* or *AKT2/AKT3* gains (Suppl. Table 1). *AKT* gains were not equally distributed between the histological subgroups: *AKT1* gain was more frequent in sarcomatoid than in epithelioid tumors (78 % vs. 36 %, $p = 0.0269$, Pearson chi-squared test), whereas gains of *AKT2* or *AKT3* were detected in epithelioid PM only. Patients' survival – analyzed in 32 patients treated with Cisplatin and Pemetrexed – was not affected by the genomic status of either AKT gene (Suppl. Fig. 2).

3.2. AKT isoforms are strongly expressed in pleural mesothelioma

We investigated the protein expression of the three AKT isoforms in primary PM specimens in order to clarify whether genomic gain of *AKT* isoforms is associated with enhanced gene expression. Immunohistochemical analyses of 91 primary PM (34 of them with known genomic status) revealed a moderate or strong protein expression of AKT1 in 66 % PM (60/91 $AKT1^{high}$), AKT2 in 80 % PM (73/91 $AKT2^{high}$) and AKT3 in 94 % PM (86/91 $AKT3^{high}$) (Fig. 1D). A total of 57 % PM co-expressed AKT1/AKT2/AKT3 (52/91 $AKT1^{high}$/$AKT2^{high}$/$AKT3^{high}$). In this cohort, each tumor was positive for at least one AKT isoform. PTEN loss, a key driver of AKT hyperactivation, was observed in 17 % (11/65) primary PM specimens (Suppl. Table 1).

Almost all (23/26) *AKT* gain events detected by OncoScan Array analysis led to increased expression of the respective AKT isoform protein (Fig. 1C, D, Suppl. Table 1). In particular, the two AKT2 gene amplifications (in tumors MPM26 and MPM36) resulted in strong AKT2 protein expression. Furthermore, AKT protein was frequently expressed in tumors with one or two AKT gene copies only, i.e. 43 % of $PM^{AKT1\ high}$, 88 % of $PM^{AKT2\ high}$ and 76 % of $PM^{AKT3\ high}$ had one/two copies of the respective AKT gene (Fig. 1D, Suppl. Table 1). As a result, despite the biased distribution of *AKT* gain events between the histological subgroups, upregulated expression of the AKT isoforms was irrespective of PM histology. Patients' survival – analyzed in 42 patients treated with Cisplatin and Pemetrexed – was not affected by the expression of either AKT isoform (Suppl. Fig. 2).

3.3. AKT inhibitor Ipatasertib decreases PM cell viability and proliferation

Next, we investigated the cytotoxic effect of the pan-AKT inhibitor Ipatasertib on PM cells. Consistent with primary patient tumors, PM cell lines PXF698, PXF1118 (both epithelioid subtype) and PXF1752 (sarcomatoid subtype) were positive for AKT3, expressing AKT3 solely (PXF1118) or in combination with AKT1 (PXF1752) or AKT2 (PXF698) (Fig. 2B). All cell lines exhibited retention of PTEN in at least 30 % cells (Suppl. Fig. 3). PM cells were exposed to increasing concentrations (0.1–10 μM) of Ipatasertib for 72 h, after which cell viability was assessed by an MTT assay. Ipatasertib impaired cell viability and proliferation in all three cell lines at submicromolar concentrations, but plateaued at 40–50 % surviving cells (Fig. 2A). The agent's efficacy was independent of the histological subtype and not enhanced when AKT1 or AKT2 was expressed in addition to AKT3. Of note, even at high concentrations of up to 10 μM, Ipatasertib did not affect the viability of non-tumor cells, i.e. fibroblasts extracted from reactive lymph nodes (Fig. 2A).

3.4. Ipatasertib induces apoptotic cell death in PM cells

To identify the mechanism of cell death induced by Ipatasertib in PM cells, we performed a real-time approach that measured the exposure of phosphatidylserine at the outer leaflet of the plasma membrane by annexin V binding as well as the loss of membrane integrity by cellular uptake of a fluorescent membrane-impermeable DNA stain. Apoptotic cell death is characterized by a delay between phosphatidylserine translocation and the loss of membrane integrity, whereas necrotic cell death is defined by concomitant annexin V binding and loss of membrane integrity. We found that Ipatasertib induced an apoptotic signature in PXF698 cells with a clear temporal lag between phosphatidylserine exposure and loss of membrane integrity of 4 h (Fig. 2C). As a control, we used Paclitaxel to induce canonical apoptotic cell death. Induction of apoptosis was confirmed by cleavage of PARP1 (poly(ADP-ribose) polymerase 1) (Fig. 2D, Suppl. Fig. 4A).

3.5. Ipatasertib acts via disrupting AKT signaling

Similar to other ATP-competitive AKT inhibitors [38,39], Ipatasertib induced a dose-dependent increase in AKT phosphorylation at the Ser473 residue in PM cells (Fig. 2E, Suppl. Fig. 4B). As shown by others, binding of ATP-competitive inhibitors to the active site of AKT can protect Ser473 from phosphatases, leading to increased p-AKT [40]. Despite this increase in p-AKT, downstream AKT signaling activity was inhibited in a dose- and time-dependent manner: Decreased PRAS40 (Thr246) and S6RP (Ser235/236) phosphorylation was observed within 4 h of treatment, maximum inhibition of both AKT targets was achieved within 24 h (Fig. 2E, 2F, Suppl. Fig. 4B). Phosphorylation of the AKT target GSK3b however, was not altered by Ipatasertib treatment of mesothelioma cells (Fig. 2F, Suppl. Fig. 4B).

3.6. Ipatasertib enhances the anti-tumor efficacy of Sapanisertib

Since the anti-tumor activity of Ipatasertib plateaued at 40–50 % of

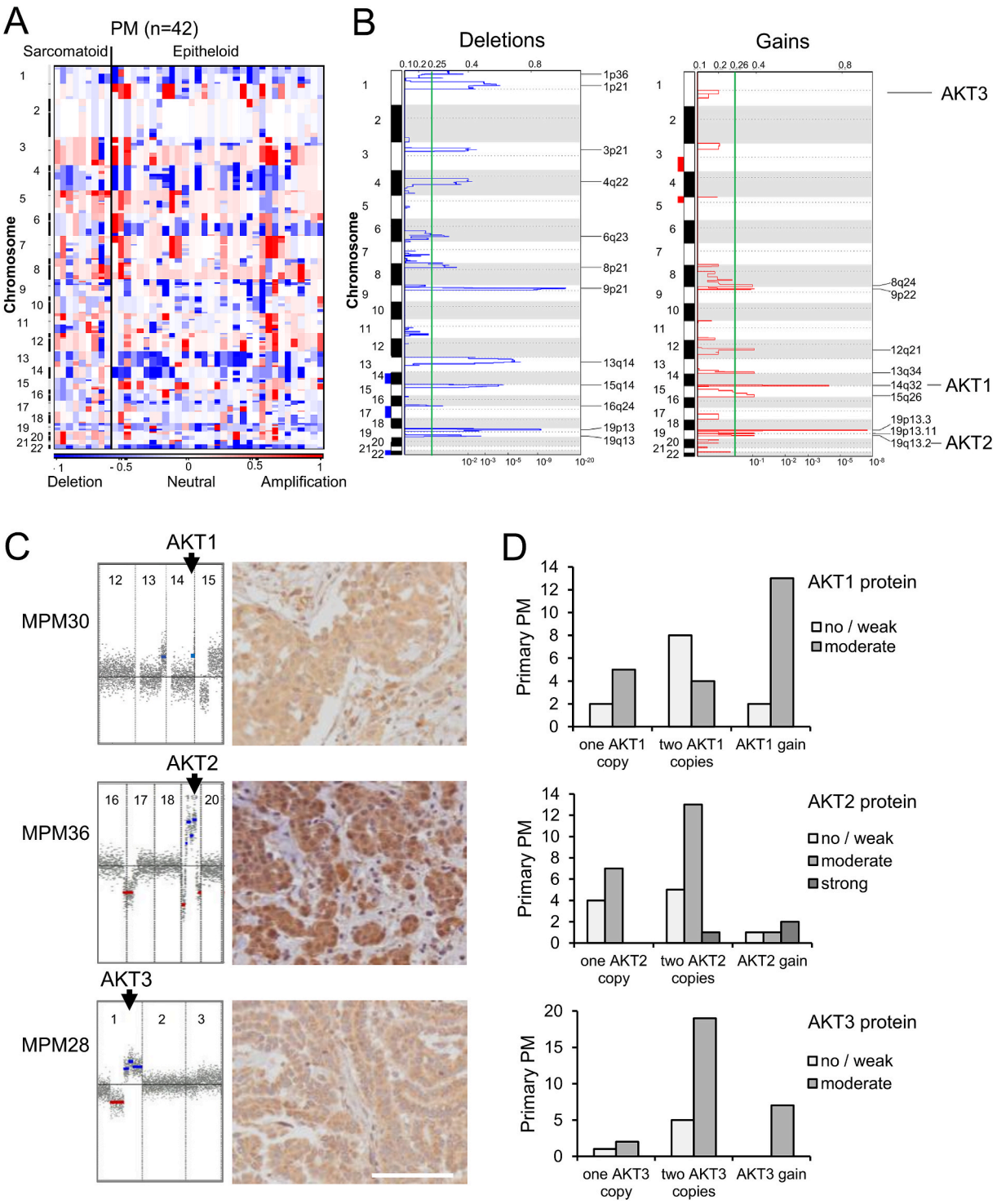

Fig. 1. AKT isoforms are present as extra-copies and overexpressed in pleural mesothelioma. (A) Heatmap showing the total segmented copy-number profile of the PM set analyzed by Oncoscan CNV array. The samples are arranged from left to right. Red and blue represent gain and loss, respectively. (B) GISTIC2.0 deletion (left) and gain (right) plots. The genome is oriented vertically from top to bottom, and GISTIC q-values at each locus are plotted from left to right on a log scale. The green line represents the significance threshold (q-value = 0.25). Broad deletion and gain events are indicated by blue and red boxes marking the chromosome regions. (C) CNV profiles and immunohistochemistry results showing the gain of *AKT1*, *AKT2* or *AKT3* and the up-regulated protein expression of the respective AKT isoforms in three primary PM. Scale, 100 μm. (D) Number of primary PM (n = 34) analyzed by Oncoscan array and AKT1, AKT2 and AKT3 immunohistochemistry and showing up-regulated protein expression in tumors with and without AKT gene gain. (For interpretation of the references to colour in this figure legend, the reader is referred to the web version of this article.)

Table 1
Significant CNV events in 42 PM specimens identified by OncoScan CNV array and GISTIC2.0.

Chromosome	Region (GRCh37.p13)	Prevalence %	Genes
Deletions			
1p36.21	chr1: 1–23.5	36 % [15/42]	*CASP9, PRDM2, PRAMEF cluster*
1p21.3	chr1: 71.9–120.4	43 % [18/42]	*DPYD*
3p21.1	chr3: 48.2–52.3	31 % [13/42]	*BAP1*
4q22.1	chr4: 88.1–88.3	45 % [19/42]	*AFF1*
6q23.2	chr6: 127.4–135.6	48 % [20/42]	*SGK1, MED23*
8p21.2	chr8: 25.7–27.8	31 % [13/42]	*ADAM7, PPP2R2A, BNIP3L, DPYSL2*
9p21.3	chr9: 21.9–22	60 % [25/42]	*CDKN2A/B, MTAP*
13q14.2	chr13: 32.9–58.2	57 % [24/42]	*RB1*
14q		38 % [16/42]	*TCL1A, FOXA1, NKX2-1, ARHGAP5, HSP90AA1*
15q14	chr15: 34.1–34.4	26 % [11/42]	*SPRED1, RASGRP1, MIR1233*
16q24.2	chr16: 86.3–90.3	21 % [9/42]	*BANP*
17		31 % [13/42]	*TP53*
19p13.2	chr19: 5.9–11.5	60 % [25/42]	*KEAP1, SMARCA4, MUC16*
19q13.41	chr19: 51.4–51.7	52 % [22/42]	*KLK cluster,SIGLEC7, SIGLEC9, CD33*
22q		74 % [31/42]	*NF2*
Gains			
3q		19 % [8/42]	*PIK3CB, PIK3CA, TNK2, CCNL1, TP63*
5p		29 % [12/42]	*TERT, CTNND2, TRIO, NKD2*
8q24.22	chr8: 128.8–146.4	24 % [10/42]	*MYC, PTK2, PTP4A3, WISP1*
9p22.2	chr9: 15.6–17.5	12 % [5/42]	*MLLT3, BNC2, CNTLN*
12q21.1	chr12: 72.1–72.4	24 % [10/42]	*RAB21*
13q34	chr13: 107.1–115.2	24 % [10/42]	*RAB20, GRK1*
14q32.33	chr14: 105.0–107.3	45 % [19/42]	*AKT1, CDCA4, MTA1*
15q26.1	chr15: 87.2–102.5	29 % [12/42]	*IGF1R, FURIN*
19p13.3	chr19: 0.3–2.5	57 % [24/42]	*STK11, APC2, MKNK2*
19p13.11	chr19: 18.3–28.3	10 % [4/42]	*JUND, PIK3R2*
19q13.2	chr19: 39–41	10 % [4/42]	*AKT2, MAP3K10, DYRK1B*

surviving tumor cells, we attempted to improve the efficacy of the drug by co-therapy with a specific inhibitor of mTOR, a key regulator of protein synthesis, proliferation and cell survival, linked with AKT signaling (Fig. 3A). The activity of mTOR is negatively regulated by the tumor suppressor NF2 (22q) deleted in 74 % of PM (Table 1). We observed an induction of moderate mTOR protein expression in 31 % (28/91) PM. In each case, mTOR was co-expressed with at least two AKT isoforms: In ten cases (11 %) with AKT2/AKT3 or AKT1/AKT3, in 19 tumors (21 %) with AKT1/AKT2/AKT3 (Suppl. Table 1).

The efficacy of a combined treatment of Ipatasertib and Sapanisertib (formerly INK128; a small molecule inhibitor of mTOR that targets both mTORC1 and mTORC2) was investigated in PM cell lines PXF698, PXF1752 and PXF1118 and in primary PM cells from two patients (MPM186, MPM187), all co-expressing mTOR and AKT. In all cases, combination treatment resulted in a more potent inhibition of cell viability compared to each drug individually (Fig. 3B). Analysis using the CompuSyn CI algorithm [37] showed that the decline in cell viability was strongly synergistic at a wide range of concentrations in all cell lines (Suppl. Fig. 6). To provide a control, we tested Met-5A cells; these showed weak AKT expression and low sensitivity to Ipatasertib. Interestingly, this level of expression still allowed Ipatasertib to enhance Sapanisertib efficacy by up to 18 % (Suppl. Fig. 7). Notably, combined Ipatasertib/Sapanisertib treatment was effectively cytotoxic in PM cells with poor chemotherapy response: PXF698, PXF1752 and MPM186 were resistant to Cisplatin; PXF1118 and MPM187 cells were sensitive to high concentrations of Cisplatin only (Suppl. Fig. 8).

Next, we explored the *in vivo* anti-tumor efficacy of simultaneous inhibition of AKT and mTOR by assessing the effect of Ipatasertib and Sapanisertib therapy on the growth of a patient-derived xenograft with AKT/mTOR co-activation and retained PTEN. As shown in Fig. 3C, Ipatasertib alone did not exert significant anti-tumor growth activity on PDX1752 grafts (sarcomatoid PM), but enhanced the anti-tumor effect of Sapanisertib causing tumor growth inhibition (TGI) of 60.1 % ($p = 0.0027$) vs. 43.9 % ($p = 0.0242$) by Sapanisertib alone. Ipatasertib, Sapanisertib and combined administrations were all well tolerated, as determined by stable body weights throughout the treatment period (Suppl. Fig. 9).

3.7. Combined Ipatasertib/Sapanisertib treatment impairs AKT/mTOR signaling and the glycolytic pathway

To gain insight into the impact of Ipatasertib/Sapanisertib co-treatment on AKT/mTOR signaling, we evaluated AKT and mTOR activation in cell lines and primary cells using immunoblotting and a bioluminescent cellular immunoassay, respectively. In PM cell lines PXF698 and PXF1118, Sapanisertib alone did not affect p-AKT (Ser473) and p-PRAS40 (Thr246) levels, but enhanced the inhibitory effect of Ipatasertib on AKT, which resulted in a robust dephosphorylation of PRAS40 (Fig. 3D, Suppl. Fig. 4C). S6RP is a target of both active AKT and mTOR (Fig. 3A). Consequently, S6RP was partially dephosphorylated when Ipatasertib or Sapanisertib were administered alone and almost completely dephosphorylated after both drugs were given in combination (Fig. 3D, Suppl. Fig. 4C). Similarly, in primary PM cells (MPM186, MPM187) co-treatment significantly decreased p-S6RP levels and p-AKT levels to a higher extent than Sapanisertib or Ipatasertib as mono-drugs (Suppl. Fig. 4D). In PXF1118 cells, but not in PXF698 cells, combined Ipatasertib/Sapanisertib treatment triggered p-ERK1/2 activation (Suppl. Fig. 5). This adverse effect, typical of AKT/mTOR inhibition, appears to be dependent on the cellular context.

AKT/mTOR signaling is critically involved in the regulation of glycolysis, the major mode of glucose metabolism and source of energy in tumor cells. We explored the impact of Ipatasertib/Sapanisertib co-treatment on glycolysis and energy metabolism by assessing lactate and intracellular ATP levels in treated cell lines (PXF698, PXF1752). Both Ipatasertib and Sapanisertib attenuated lactate levels, and co-treatment caused a significant decrease of intracellular ATP (Fig. 3E). Our data suggest that the simultaneous inhibition of AKT and mTOR impairs glycolysis, which leads to ATP depletion from treated PM cells.

4. Discussion

The PI3K/AKT/mTOR signaling pathway is the most frequently activated signaling pathway in human cancer [41]. PI3K/AKT/mTOR signaling regulates tumor cell proliferation, survival, metabolism, motility and invasion, thus promoting tumor progression and metastasis [41,42]. Here, we identified all three members of the AKT serine/threonine protein kinase family as aberrantly activated oncogenes in pleural mesothelioma and demonstrate that AKT is a suitable target for the treatment of PM.

AKT activation in solid tumors is more commonly driven by gene amplifications than mutations [41,43]. This study presents the first report of recurrent gains and amplifications of *AKT1*, *AKT2*, and *AKT3* in PM. While earlier studies primarily described 14q32 *(AKT1)* losses in PM [44–46], our high-resolution SNP-based Oncoscan

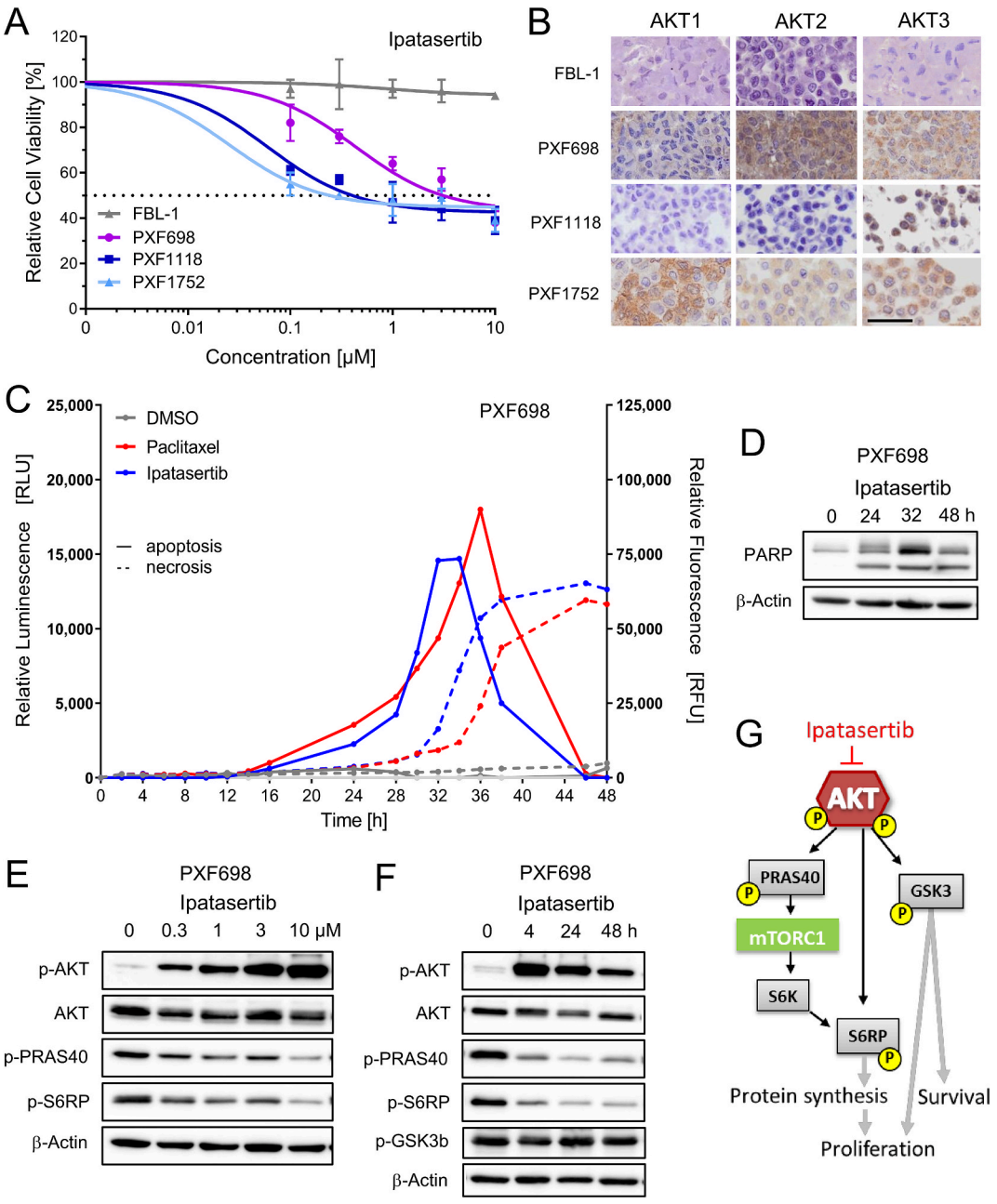

Fig. 2. Ipatasertib impairs mesothelioma cell viability. (A) PM-PDX cell lines PXF698, PXF1118 and PXF1752 and fibroblasts FBL-1 were exposed to the indicated concentrations of Ipatasertib. Cell viability was measured after 72 h of treatment by an MTT cytotoxicity assay. Data points, mean ± SD of independent triplicate experiments. (B) Immunohistochemistry analysis of AKT1, AKT2 and AKT3 protein expression in PXF698, PXF1118 and PXF1752 PM cells and fibroblasts FBL-1. Scale, 50 μm. (C) PXF698 cells were exposed to Ipatasertib (10 μM), Paclitaxel (400 nM) or DMSO in the presence of the RealTime-Glo Annexin V Apoptosis and Necrosis Assay. Luminescence (phosphatidyl:annexin V binding – apoptosis; solid line) and fluorescence (loss of membrane integrity – necrosis; dashed line) were recorded for 48 h at the indicated time points. A clear temporal lag between phosphatidylserine exposure and lack of membrane integrity is indicative of apoptotic cell death leading to secondary necrosis. Data points, mean of duplicate samples, representative of independent duplicate experiments. (D) PARP1 cleavage after treatment of PXF698 cells with 10 μM Ipatasertib; uncleaved PARP1 (116 kD), PARP1 carboxy-terminal catalytic domain (89 kD). (E) Immunoblot analysis of AKT pathway components p-AKT (Ser473), p-PRAS40 (Thr246), and p-RPS6 (Ser235/236) in response to increasing concentrations of Ipatasertib in PXF698 after 24 h of treatment. (F) Levels of p-AKT (Ser473), p-PRAS40 (Thr246), p-RPS6 (Ser235/236), and p-GSK3b (Ser9) in PXF698 cells after 10 μM Ipatasertib treatment at 0, 4, 24, 48 h. (G) Schematic illustration of AKT signaling.

analysis—combined with GISTIC2.0—uncovered small (2–8 Mb) 14q32 gains encompassing *AKT1*. Sporadic gains at this locus have been observed in other PM studies using high-resolution arrays [8,47], and occasional gains of 1q43 *(AKT3)* [46,48,49] or 19q13 *(AKT2)* [47–49] have also been reported. The differences between our findings and earlier reports likely stem from methodological distinctions: (1) Our Oncoscan and GISTIC2.0 platform allowed detection of small-scale *AKT1* CNVs, whereas prior studies using lower-resolution microarrays (e.g., CGH or arrayCGH) may have missed focal gains; (2) In our cohort, two of four *AKT2* gains were high-level amplifications (four or more copies) – a feature prioritized by GISTIC2.0 due to its potential biological significance. These factors likely explain why our study identified recurrent gains in *AKT1*, *AKT2*, and *AKT3*, while others observed only sporadic aberrations.

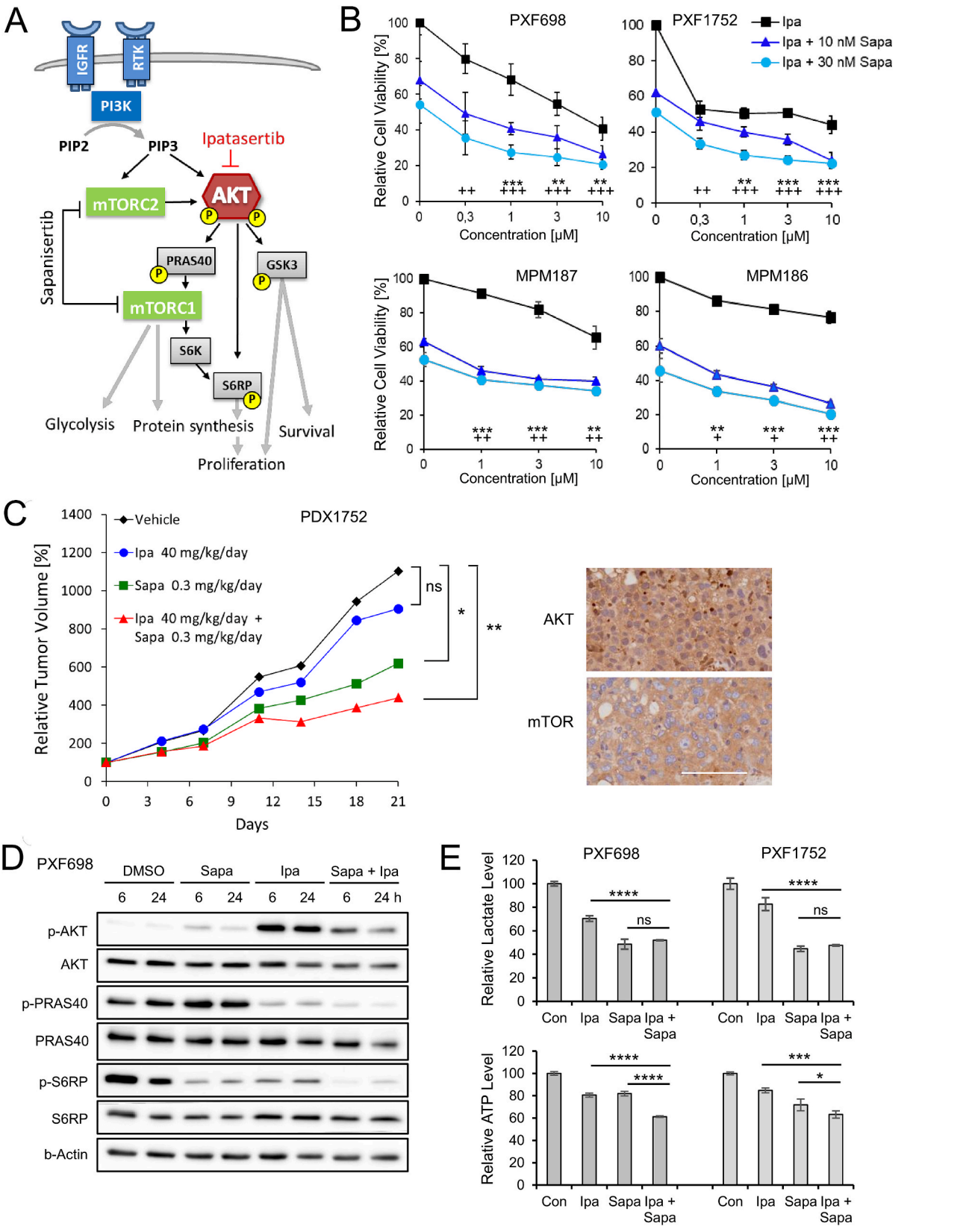

(caption on next page)

Fig. 3. Synergistic cytotoxicity of Ipatasertib (AKT inhibitor) and Sapanisertib (mTORC1/2 inhibitor). (A) Schematic illustration of PI3K/AKT/mTOR signaling. Growth factors and hormones activate PI3 kinase catalyzing the production of PIP3, which in turn coordinates glycolysis, cell proliferation, and survival via activating AKT and mTOR signaling pathways. mTOR kinase serves as core component of two distinct protein complexes, mTORC1 and mTORC2. (B) Impact of Ipatasertib, Sapanisertib, or their combinations on the viability of PM-PDX cell lines (PXF698, epithelioid; PXF1752, sarcomatoid) and primary PM cells (MPM186, MPM187; both epitheliod). **p < 0.01, ***p < 0.001 vs. Ipa alone and 10 nM Sapa; +p < 0.05, ++p < 0.01, +++p < 0.001 vs. Ipa alone and 30 nM Sapa after 72 h therapy (one-way ANOVA). (C) *In vivo* efficacy of Ipatasertib, Sapanisertib and combined treatment in mesothelioma xenograft model PDX1752 (sarcomatoid). Changes in the tumor volume over the time course of the experiment relative to day 0 of treatment. *p < 0.05, **p < 0.01, ns = not significant (one-way ANOVA). Up-regulated AKT and mTOR protein expression in the xenograft tumor tissue; scale, 100 μm. (D) Molecular effects of AKT and mTOR inhibition. Levels of p-AKT (Ser473), p-PRAS40 (Thr246), and p-RPS6 (Ser235/236) in PXF698 cells treated with 10 μM Ipatasertib, 30 nM Sapanisertib, or their combination for 6 h and 24 h. (E) ATP and lactate levels in PM-PDX cell lines (PXF698, PXF1752) after treatment with 10 μM Ipatasertib, 30 nM Sapanisertib, or their combination for 24 h. *p < 0.05, ***p < 0.001, ****p < 0.0001, ns = not significant (one-way ANOVA).

A large number (88 %) of *AKT* gain events were associated with an enhanced expression of the respective AKT isoform protein. Beyond that, AKT isoform protein expression was also frequently upregulated in tumors with one or two AKT gene copies only, which altogether resulted in an upregulated expression of AKT1, AKT2 and AKT3 in 66 %, 80 % and 94 % PM, respectively. Our observation of AKT protein expression in the vast majority of PM tumors is in line with previous reports on AKT1 and AKT3 expression in PM cell lines [29] and upregulated expression of phosphorylated AKT in 65–88 % PM [26–28].

Despite sharing 80 % structural similarity, the three AKT isoforms exert non-redundant and occasionally opposing effects on tumor pathogenesis. Generally, AKT1 drives tumor initiation and cell proliferation by regulating the cell cycle and inhibiting p53-mediated apoptosis, yet it decreases cell migration [42,50]. Conversely, AKT2 promotes tumor progression, migration, and invasion by regulating β-integrins, EMT-proteins and F-actin – making it a well-established mediator of metastasis, such as in breast cancer [42,50]. AKT3 exhibits pro-proliferative and pro-oncogenic properties but anti-metastatic effects [42,51]. While both AKT1 and AKT3 stimulate angiogenesis, all three isoforms converge to upregulate tumor metabolism, in particular glycolysis [52]. Notably, although AKT2 is a well-established driver of metastasis in other cancers [50], its protein expression did not correlate with metastatic events in our PM cohort.

Targeting the tumor-promoting function of AKT, the pan-AKT inhibitor Ipatasertib decreased cell viability and induced apoptotic cell death in PM cells that expressed AKT1/AKT3, AKT2/AKT3 or AKT3 solely. Ipatasertib's efficacy was independent of the histological subtype and not enhanced when AKT1 or AKT2 was expressed in addition to AKT3. Given that AKT3 protein expression was elevated in 94 % of PM cases, Ipatasertib presents a promising treatment option for the vast majority of tumors, regardless of the histological subtype.

Previous investigations of specific AKT inhibitors in PM cell lines demonstrated sensitivity to both allosteric (Perifosine) and ATP-competitive AKT inhibitors (Ipatasertib, Afuresertib, AZD5363/Capivasertib) [29,30]. However, as single agents, their cell killing efficacies were modest [29,30]. Our findings revealed that combining Ipatasertib with the mTOR inhibitor Sapanisertib enhanced cytotoxicity in PM cell lines, patient derived cells and in an *in vivo* model. This suggests a cooperative effect in inactivating the PI3K/AKT/mTOR signaling pathway. Notably, the combination showed comparable efficacy in both epithelioid and sarcomatoid PM cell lines and demonstrated activity in a sarcomatoid PDX model. Despite the limited dataset, these findings suggest that dual AKT/mTOR inhibition could be effective for both histological subtypes. Supporting this, dual targeting of PI3K/AKT/mTOR – achieved by combining AKT knockdown with the mTORC1 inhibitor RAD001 (Everolimus) – had a greater effect on mesothelioma proliferation and viability than either approach alone [53]. Additionally, studies in breast cancer cells and in *in vivo* models of non-Hodgkin lymphomas have shown synergistic antitumor activity with combined AKT and mTOR inhibitors [54,55]. In line with those studies, Ipatasertib/Sapanisertib co-treatment was well tolerated by *in vivo* PM models. Given that 31 % of PM cases in our cohort co-expressed both therapy targets, this combination therapy could benefit approximately one-third of PM patients.

Deletion of the tumor suppressor NF2 gene, a key genomic alteration implicated in the pathogenesis of PM [10], was detected in 74 % of our PM cohort. NF2 inactivation leads to mTOR hyperactivation, which promotes oncogenic protein, lipid and nucleotide synthesis, glycolysis, cell proliferation and survival [10,11,56]. While mTORC1 inhibition by rapamycin derivatives suppressed PM cell growth in preclinical models [11,13,14], clinical trials (e.g., NCT01024946) [15] showed limited efficacy due to AKT reactivation – a consequence of disrupted negative feedback from mTOR to PI3K [57]. Our study demontrated that Ipatasertib synergized with Sapanisertib to inactivate AKT – indicated by robust dephosphorylation of the AKT key substrate PRAS40. This dual inhibition prevented mTORC2-mediated AKT reactivation.

S6RP, a critical effector of PI3K/AKT/mTOR-drivenprotein synthesis and proliferation, was partially dephosphorylated with either agent alone but almost completely inactivated upon co-treatment. This indicates a robust blockade of PI3K/AKT/mTOR signaling, whereas single-agent treatment left the pathway partially active. These results align with recent reports showing that AKT and mTORC1 co-inhibition suppresses AKT and RPS6 phosphorylation in breast cancer and non-Hodgkin lymphoma models [54,55].

Beyond pathway inhibition, Ipatasertib/Sapanisertib co-treatment disrupted tumor cell energy metabolism, reducing glycolysis and synergistically lowering intracellular ATP levels. This aligns with the known roles of AKT isoforms and mTOR in promoting glycolysis in tumor cells [52,56]. Taken together, the Ipatasertib/Sapanisertib combination had two major effects: (1) impaired PI3K/AKT/mTOR survival signaling; (2) suppressed energy metabolism. We hypothesize that the blockade of survival signals and energy depletion cooperate to impair cell growth and survival and to induce apoptotic cell death.

This report represents an initial step in evaluating the therapeutic potential of dual AKT and mTOR inhibition as a treatment strategy for PM, warranting further experimental and clinical validation. Of particular interest is assessing the anti-tumor potential of Capivasertib, an alternative pan-AKT inhibitor, in PM. Both Ipatasertib and Capivasertib are orally administered small-molecule inhibitors targeting all three AKT isoforms and demonstrated comparable anti-tumor efficacy in early clinical trials [39,58–60]. However, Phase III trials in breast cancer showed only modest benefits for Ipatasertib plus Paclitaxel, [61] leading Roche to discontinue its development, leaving no clinical prospects for mesothelioma. In contrast, Capivasertib in combination with the estrogen-receptor degrader Fulvestrant distinctly improved progression-free survival compared to Fulvestrant alone [62]. This success led to its FDA approval for breast cancer treatment [63]. Given its efficacy in tumors with PIK3CA/AKT1/PTEN alterations, we aim to investigate Capivasertib's potential in mesothelioma. Since PTEN loss is a key driver of AKT hyperactivation, whether through increase in PIP3 levels or as EPHA2/SRC downstream target, our study will specifically focus on PTEN-loss/AKT-positive tumors, which constituted 17 % of our patient cohort.

5. Conclusions

All three isoformes of the AKT kinase are widely activated in pleural mesothelioma by copy number gain and/or upregulated expression.

Simultaneous pharmacological inactivation of AKT and mTOR in experimental PM models exhibits synergistic antitumor activity and should be further explored as a targeted therapeutic alternative in mesothelioma.

CRediT authorship contribution statement

Claudia Kalla: Writing – review & editing, Writing – original draft, Visualization, Validation, Supervision, Project administration, Methodology, Funding acquisition, Data curation, Conceptualization. **Dina Mönch:** Writing – review & editing, Writing – original draft, Validation, Methodology, Investigation, Formal analysis. **Sophia Steinlein:** Writing – review & editing, Methodology, Investigation, Funding acquisition. **Alessandro Pastore:** Writing – review & editing, Software, Methodology, Formal analysis, Data curation. **Heike Horn:** Writing – review & editing, Resources. **Roger Falkenstern-Ge:** Writing – review & editing, Resources. **Julia Schüler:** Writing – review & editing, Methodology. **German Ott:** Writing – review & editing, Writing – original draft, Supervision, Funding acquisition, Formal analysis, Conceptualization. **Gerhard Preissler:** Writing – review & editing, Writing – original draft, Resources, Funding acquisition, Conceptualization.

Funding

The study was supported by the Robert Bosch Stiftung, Stuttgart, Germany (Projects 704, 796 and 7101).

Declaration of competing interest

The authors declare the following financial interests/personal relationships which may be considered as potential competing interests: AP is an employee of Novartis Institutes for BioMedical Research. All other authors declare no conflicts of interest.

Acknowledgments

We thank Sabine Bode-Erdmann, Robert Bosch Hospital Stuttgart, for expert histological diagnosis and Katja Bräutigam, IKP Stuttgart, for excellent technical assistance. The study was supported by the Robert Bosch Stiftung, Stuttgart, Germany (Projects 704, 796 and 7101).

Appendix A. Supplementary data

Supplementary data to this article can be found online at https://doi.org/10.1016/j.lungcan.2026.109512.

References

[1] C. Cao, D. Tian, C. Manganas, P. Matthews, T.D. Yan, Systematic review of trimodality therapy for patients with malignant pleural mesothelioma, Ann Cardiothorac Surg 1 (2012) 428–437, https://doi.org/10.3978/j.issn.2225-319X.2012.11.07.

[2] G. Cardillo, D. Waller, S. Tenconi, V. Di Noia, S. Ricciardi, Malignant Pleural Mesothelioma: a 2025 Update, J. Clin. Med. 14 (2025) 1004, https://doi.org/10.3390/jcm14031004.

[3] A. Scherpereel, P. Astoul, P. Baas, T. Berghmans, H. Clayson, P. de Vuyst, H. Dienemann, F. Galateau-Salle, C. Hennequin, G. Hillerdal, C. Le Péchoux, L. Mutti, J.-C. Pairon, R. Stahel, P. van Houtte, J. van Meerbeeck, D. Waller, W. Weder, European respiratory society/european society of thoracic surgeons task force, guidelines of the european respiratory society and the european society of thoracic surgeons for the management of malignant pleural mesothelioma, Eur. Respir. J. 35 (2010) 479–495, https://doi.org/10.1183/09031936.00063109.

[4] A. Scherpereel, I. Opitz, T. Berghmans, I. Psallidas, M. Glatzer, D. Rigau, P. Astoul, S. Bölükbas, J. Boyd, J. Coolen, C.D. Bondt, D.D. Ruysscher, V. Durieux, C. Faivre-Finn, D. Fennell, F. Galateau-Salle, L. Greillier, M.A. Hoda, W. Klepetko, A. Lacourt, P. McElnay, N.A. Maskell, L. Mutti, J.-C. Pairon, P.V. Schil, J.P. van Meerbeeck, D. Waller, W. Weder, G. Cardillo, P.M. Putora, ERS/ESTS/EACTS/ESTRO guidelines for the management of malignant pleural mesothelioma, Eur. Respir. J. (2020), https://doi.org/10.1183/13993003.00953-2019.

[5] S. Peters, A. Scherpereel, R. Cornelissen, Y. Oulkhouir, L. Greillier, M.A. Kaplan, T. Talbot, I. Monnet, S. Hiret, P. Baas, A.K. Nowak, N. Fujimoto, A.S. Tsao, A. S. Mansfield, S. Popat, X. Zhang, N. Hu, D. Balli, T. Spires, G. Zalcman, First-line nivolumab plus ipilimumab versus chemotherapy in patients with unresectable malignant pleural mesothelioma: 3-year outcomes from CheckMate 743, Ann. Oncol. 33 (2022) 488–499, https://doi.org/10.1016/j.annonc.2022.01.074.

[6] P. Baas, A. Scherpereel, A.K. Nowak, N. Fujimoto, S. Peters, A.S. Tsao, A. S. Mansfield, S. Popat, T. Jahan, S. Antonia, Y. Oulkhouir, Y. Bautista, R. Cornelissen, L. Greillier, F. Grossi, D. Kowalski, J. Rodríguez-Cid, P. Aanur, A. Oukessou, C. Baudelet, G. Zalcman, First-line nivolumab plus ipilimumab in unresectable malignant pleural mesothelioma (CheckMate 743): a multicentre, randomised, open-label, phase 3 trial, Lancet 397 (2021) 375–386, https://doi.org/10.1016/S0140-6736(20)32714-8.

[7] S. Popat, P. Baas, C. Faivre-Finn, N. Girard, A.G. Nicholson, A.K. Nowak, I. Opitz, A. Scherpereel, M. Reck, Malignant pleural mesothelioma: ESMO Clinical Practice guidelines for diagnosis, treatment and follow-up☆, Ann. Oncol. 33 (2022) 129–142, https://doi.org/10.1016/j.annonc.2021.11.005.

[8] M. Bott, M. Brevet, B.S. Taylor, S. Shimizu, T. Ito, L. Wang, J. Creaney, R.A. Lake, M.F. Zakowski, B. Reva, C. Sander, R. Delsite, S. Powell, Q. Zhou, R. Shen, A. Olshen, V. Rusch, M. Ladanyi, The nuclear deubiquitinase BAP1 is commonly inactivated by somatic mutations and 3p21.1 losses in malignant pleural mesothelioma, Nat. Genet. 43 (2011) 668–672, https://doi.org/10.1038/ng.855.

[9] P.B. Illei, V.W. Rusch, M.F. Zakowski, M. Ladanyi, Homozygous deletion of CDKN2A and codeletion of the methylthioadenosine phosphorylase gene in the majority of pleural mesotheliomas, Clin. Cancer Res. 9 (2003) 2108–2113.

[10] T. Sato, Y. Sekido, NF2/Merlin Inactivation and potential Therapeutic Targets in Mesothelioma, Int. J. Mol. Sci. 19 (2018) 988, https://doi.org/10.3390/ijms19040988.

[11] M.A. López-Lago, T. Okada, M.M. Murillo, N. Socci, F.G. Giancotti, Loss of the tumor suppressor gene NF2, encoding merlin, constitutively activates integrin-dependent mTORC1 signaling, Mol. Cell Biol. 29 (2009) 4235–4249, https://doi.org/10.1128/MCB.01578-08.

[12] R.A. Saxton, D.M. Sabatini, mTOR Signaling in growth, Metabolism, and Disease, Cell 168 (2017) 960–976, https://doi.org/10.1016/j.cell.2017.02.004.

[13] M.-L. Hartman, J.M. Esposito, B.Y. Yeap, D.J. Sugarbaker, Combined treatment with cisplatin and sirolimus to enhance cell death in human mesothelioma, J. Thorac. Cardiovasc. Surg. 139 (2010) 1233–1240, https://doi.org/10.1016/j.jtcvs.2009.06.027.

[14] M.A. Hoda, A. Mohamed, B. Ghanim, M. Filipits, B. Hegedus, M. Tamura, J. Berta, B. Kubista, B. Dome, M. Grusch, U. Setinek, M. Micksche, W. Klepetko, W. Berger, Temsirolimus Inhibits Malignant Pleural Mesothelioma Growth In Vitro and In Vivo: Synergism with Chemotherapy, J. Thorac. Oncol. 6 (2011) 852–863, https://doi.org/10.1097/JTO.0b013e31820e1a25.

[15] S.-H.-I. Ou, J. Moon, L.L. Garland, P.C. Mack, J.R. Testa, A.S. Tsao, A.J. Wozniak, D.R. Gandara, SWOG S0722: phase II study of mTOR inhibitor everolimus (RAD001) in advanced malignant pleural mesothelioma (MPM), J. Thorac. Oncol. 10 (2015) 387–391, https://doi.org/10.1097/JTO.0000000000000360.

[16] M. Brevet, S. Shimizu, M.J. Bott, N. Shukla, Q. Zhou, A.B. Olshen, V. Rusch, M. Ladanyi, Coactivation of receptor tyrosine kinases in malignant mesothelioma as a rationale for combination targeted therapy, J. Thorac. Oncol. 6 (2011) 864–874.

[17] C.W. Menges, Y. Chen, B.T. Mossman, J. Chernoff, A.T. Yeung, J.R. Testa, A Phosphotyrosine Proteomic Screen Identifies Multiple Tyrosine Kinase Signaling Pathways Aberrantly Activated in Malignant Mesothelioma, Genes, Cancer 1 (2010) 493–505, https://doi.org/10.1177/1947601910375273.

[18] L.A. Marek, T.K. Hinz, A. von Mässenhausen, K.A. Olszewski, E.K. Kleczko, D. Boehm, M.C. Weiser-Evans, R.A. Nemenoff, H. Hoffmann, A. Warth, J.M. Gozgit, S. Perner, L.E. Heasley, Nonamplified FGFR1 is a growth driver in malignant pleural mesothelioma, Mol. Cancer Res. 12 (2014) 1460–1469, https://doi.org/10.1158/1541-7786.MCR-14-0038.

[19] R. Kanteti, I. Dhanasingh, I. Kawada, F.E. Lennon, Q. Arif, R. Bueno, R. Hasina, A. N. Husain, W. Vigneswaran, T. Seiwert, H.L. Kindler, R. Salgia, MET and PI3K/mTOR as a potential Combinatorial Therapeutic Target in Malignant Pleural Mesothelioma, PLoS One 9 (2014), https://doi.org/10.1371/journal.pone.0105919.

[20] K. Kawaguchi, H. Murakami, T. Taniguchi, M. Fujii, S. Kawata, T. Fukui, Y. Kondo, H. Osada, N. Usami, K. Yokoi, Y. Ueda, Y. Yatabe, M. Ito, Y. Horio, T. Hida, Y. Sekido, Combined inhibition of MET and EGFR suppresses proliferation of malignant mesothelioma cells, Carcinogenesis 30 (2009) 1097–1105, https://doi.org/10.1093/carcin/bgp097.

[21] R. Masood, A. Kundra, S. Zhu, G. Xia, P. Scalia, D.L. Smith, P.S. Gill, Malignant mesothelioma growth inhibition by agents that target the VEGF and VEGF-C autocrine loops, Int. J. Cancer 104 (2003) 603–610, https://doi.org/10.1002/ijc.10996.

[22] L.L. Garland, K. Chansky, A.J. Wozniak, A.S. Tsao, S.M. Gadgeel, C. F. Verschraegen, M.A. DaSilva, M. Redman, D.R. Gandara, Phase II Study of AZD2171 in patients with Malignant Pleural Mesothelioma: SWOG S0509, J. Thorac. Oncol. 6 (2011) 1938–1945, https://doi.org/10.1097/JTO.0b013e318229586e.

[23] S.A. Laurie, D. Hao, N.B. Leighl, J. Goffin, A. Khomani, A. Gupta, C.L. Addison, A. Bane, J. Seely, M.L. Filion, G.R. Pond, M.N. Levine, A phase II trial of dovitinib in previously-treated advanced pleural mesothelioma: the Ontario Clinical Oncology Group, Lung Cancer 104 (2017) 65–69, https://doi.org/10.1016/j.lungcan.2016.12.004.

[24] R. Govindan, R.A. Kratzke, J.E. Herndon, G.A. Niehans, R. Vollmer, D. Watson, M. R. Green, H.L. Kindler, Cancer and Leukemia Group B (CALGB 30101), Gefitinib in patients with malignant mesothelioma: a phase II study by the Cancer and

Leukemia Group B, Clin. Cancer Res. 11 (2005) 2300–2304, https://doi.org/10.1158/1078-0432.CCR-04-1940.
[25] L.L. Garland, C. Rankin, D.R. Gandara, S.E. Rivkin, K.M. Scott, R.B. Nagle, A.J. P. Klein-Szanto, J.R. Testa, D.A. Altomare, E.C. Borden, Phase II study of erlotinib in patients with malignant pleural mesothelioma: a Southwest Oncology Group Study, J. Clin. Oncol. 25 (2007) 2406–2413, https://doi.org/10.1200/JCO.2006.09.7634.
[26] S.B. Watzka, U. Setinek, E.B. Stubenberger, M. Tötsch, G. Dekan, M. Marcher, T. Fleck, M.R. Müller, Integrin-linked kinase, phosphorylated AKT and the prognosis of malignant pleural mesothelioma, Eur. J. Cardiothorac. Surg. 39 (2011) 180–184, https://doi.org/10.1016/j.ejcts.2010.05.007.
[27] D.A. Altomare, H. You, G.-H. Xiao, M.E. Ramos-Nino, K.L. Skele, A. De Rienzo, S. C. Jhanwar, B.T. Mossman, A.B. Kane, J.R. Testa, Human and mouse mesotheliomas exhibit elevated AKT/PKB activity, which can be targeted pharmacologically to inhibit tumor cell growth, Oncogene 24 (2005) 6080–6089, https://doi.org/10.1038/sj.onc.1208744.
[28] S. Cedrés, M.A. Montero, P. Martinez, A. Martinez, V. Rodríguez-Freixinós, D. Torrejon, A. Gabaldon, M. Salcedo, S. Ramon Y Cajal, E. Felip, Exploratory analysis of activation of PTEN-PI3K pathway and downstream proteins in malignant pleural mesothelioma (MPM), Lung Cancer 77 (2012) 192–198. https://doi.org/10.1016/j.lungcan.2012.02.022.
[29] G. Pinton, A.G. Manente, G. Angeli, L. Mutti, L. Moro, Perifosine as a potential novel anti-cancer agent inhibits EGFR/MET-AKT axis in malignant pleural mesothelioma, PLoS One 7 (2012) e36856, https://doi.org/10.1371/journal.pone.0036856.
[30] M. Yamaji, A. Ota, M. Wahiduzzaman, S. Karnan, T. Hyodo, H. Konishi, S. Tsuzuki, Y. Hosokawa, M. Haniuda, Novel ATP-competitive Akt inhibitor afuresertib suppresses the proliferation of malignant pleural mesothelioma cells, Cancer Med. 6 (2017) 2646–2659, https://doi.org/10.1002/cam4.1179.
[31] A.M. Staiger, J. Duppel, M.A. Dengler, H. van der Kuip, M.C. Vöhringer, W. E. Aulitzky, A. Rosenwald, G. Ott, H. Horn, An analysis of the role of follicular lymphoma-associated fibroblasts to promote tumor cell viability following drug-induced apoptosis, Leuk. Lymphoma 58 (2017) 1922–1930, https://doi.org/10.1080/10428194.2016.1263841.
[32] F. Commo, J. Guinney, C. Ferté, B. Bot, C. Lefebvre, J.-C. Soria, F. André, rCGH: a comprehensive array-based genomic profile platform for precision medicine, Bioinformatics 32 (2016) 1402–1404, https://doi.org/10.1093/bioinformatics/btv718.
[33] C.H. Mermel, S.E. Schumacher, B. Hill, M.L. Meyerson, R. Beroukhim, G. Getz, GISTIC2.0 facilitates sensitive and confident localization of the targets of focal somatic copy-number alteration in human cancers, Genome Biol. 12 (2011) R41, https://doi.org/10.1186/gb-2011-12-4-r41.
[34] K. Gruber, H. Horn, J. Kalla, P. Fritz, A. Rosenwald, M. Kohlhäufl, G. Friedel, M. Schwab, G. Ott, C. Kalla, Detection of rearrangements and transcriptional up-regulation of ALK in FFPE lung cancer specimens using a novel, sensitive, quantitative reverse transcription polymerase chain reaction assay, J. Thorac. Oncol. 9 (2014) 307–315, https://doi.org/10.1097/JTO.0000000000000068.
[35] N. Fusco, E. Guerini-Rocco, I. Castellano, U. Malapelle, Immunohistochemistry for PTEN testing in HR +/HER2- metastatic breast cancer, Virchows Arch. 487 (2025) 727–732, https://doi.org/10.1007/s00428-025-04249-5.
[36] D. Mönch, S. Bode-Erdmann, J. Kalla, J. Sträter, C. Schwänen, R. Falkenstern-Ge, S. Klumpp, G. Friedel, G. Ott, C. Kalla, A subgroup of pleural mesothelioma expresses ALK protein and may be targetable by combined rapamycin and crizotinib therapy, Oncotarget 9 (2018) 20781–20794, https://doi.org/10.18632/oncotarget.25111.
[37] T.-C. Chou, Theoretical Basis, Experimental Design, and Computerized simulation of Synergism and Antagonism in Drug Combination Studies, Pharmacol. Rev. 58 (2006) 621–681, https://doi.org/10.1124/pr.58.3.10.
[38] T. Okuzumi, D. Fiedler, C. Zhang, D.C. Gray, B. Aizenstein, R. Hoffman, K. M. Shokat, Inhibitor hijacking of Akt activation, Nat. Chem. Biol. 5 (2009) 484–493, https://doi.org/10.1038/nchembio.183.
[39] J. Lin, D. Sampath, M.A. Nannini, B.B. Lee, M. Degtyarev, J. Oeh, H. Savage, Z. Guan, R. Hong, R. Kassees, L.B. Lee, T. Risom, S. Gross, B.M. Liederer, H. Koeppen, N.J. Skelton, J.J. Wallin, M. Belvin, E. Punnoose, L.S. Friedman, K. Lin, Targeting Activated Akt with GDC-0068, a Novel Selective Akt Inhibitor that is Efficacious in Multiple Tumor Models, Clin. Cancer Res. 19 (2013) 1760–1772, https://doi.org/10.1158/1078-0432.CCR-12-3072.
[40] K. Lin, J. Lin, W.-I. Wu, J. Ballard, B.B. Lee, S.L. Gloor, G.P.A. Vigers, T.H. Morales, L.S. Friedman, N. Skelton, B.J. Brandhuber, An ATP-Site On-off Switch that Restricts Phosphatase Accessibility of Akt, Science Signaling 5 (2012) ra37–ra37, https://doi.org/10.1126/scisignal.2002618.
[41] A. Glaviano, A.S.C. Foo, H.Y. Lam, K.C.H. Yap, W. Jacot, R.H. Jones, H. Eng, M. G. Nair, P. Makvandi, B. Geoerger, M.H. Kulke, R.D. Baird, J.S. Prabhu, D. Carbone, C. Pecoraro, D.B.L. Teh, G. Sethi, V. Cavalieri, K.H. Lin, N.R. Javidi-Sharifi, E. Toska, M.S. Davids, J.R. Brown, P. Diana, J. Stebbing, D.A. Fruman, A.P. Kumar, PI3K/AKT/mTOR signaling transduction pathway and targeted therapies in cancer, Mol. Cancer 22 (2023) 138, https://doi.org/10.1186/s12943-023-01827-6.
[42] S.E. Degan, I.H. Gelman, Emerging Roles for AKT Isoform Preference in Cancer Progression Pathways, Mol. Cancer Res. 19 (2021) 1251–1257, https://doi.org/10.1158/1541-7786.MCR-20-1066.
[43] D.A. Altomare, J.R. Testa, Perturbations of the AKT signaling pathway in human cancer, Oncogene 24 (2005) 7455–7464, https://doi.org/10.1038/sj.onc.1209085.
[44] M. Takeda, T. Kasai, Y. Enomoto, M. Takano, K. Morita, T. Nakai, N. Iizuka, H. Maruyama, C. Ohbayashi, Comparison of genomic abnormality in malignant mesothelioma by the site of origin, J. Clin. Pathol. 67 (2014) 1038–1043, https://doi.org/10.1136/jclinpath-2014-202465.
[45] T. Taniguchi, S. Karnan, T. Fukui, T. Yokoyama, H. Tagawa, K. Yokoi, Y. Ueda, T. Mitsudomi, Y. Horio, T. Hida, Y. Yatabe, M. Seto, Y. Sekido, Genomic profiling of malignant pleural mesothelioma with array-based comparative genomic hybridization shows frequent non-random chromosomal alteration regions including JUN amplification on 1p32, Cancer Sci. 98 (2007) 438–446, https://doi.org/10.1111/j.1349-7006.2006.00386.x.
[46] A.M. Björkqvist, L. Tammilehto, S. Anttila, K. Mattson, S. Knuutila, Recurrent DNA copy number changes in 1q, 4q, 6q, 9p, 13q, 14q and 22q detected by comparative genomic hybridization in malignant mesothelioma, Br. J. Cancer 75 (1997) 523–527, https://doi.org/10.1038/bjc.1997.91.
[47] G. Serio, L. Vimercati, A. Pennella, M. Gentile, D. Cavone, A.L. Buonadonna, A. Scattone, F. Fortarezza, A. De Palma, A. Marzullo, Genomic changes of chromosomes 8p23.1 and 1q21: Novel mutations in malignant mesothelioma, Lung Cancer 126 (2018) 106–111, https://doi.org/10.1016/j.lungcan.2018.10.012.
[48] M. Hylebos, G. Van Camp, G. Vandeweyer, E. Fransen, M. Beyens, R. Cornelissen, A. Suls, P. Pauwels, J.P. van Meerbeeck, K. Op de Beeck, Large-scale copy number analysis reveals variations in genes not previously associated with malignant pleural mesothelioma, Oncotarget 8 (2017) 113673–113686, https://doi.org/10.18632/oncotarget.22817.
[49] P.M. Lindholm, K. Salmenkivi, H. Vauhkonen, A.G. Nicholson, S. Anttila, V. L. Kinnula, S. Knuutila, Gene copy number analysis in malignant pleural mesothelioma using oligonucleotide array CGH, Cytogenet. Genome Res. 119 (2007) 46–52, https://doi.org/10.1159/000109618.
[50] N. Hinz, M. Jücker, Distinct functions of AKT isoforms in breast cancer: a comprehensive review, Cell Commun. Signaling 17 (2019) 154, https://doi.org/10.1186/s12964-019-0450-3.
[51] I. Hers, E.E. Vincent, J.M. Tavaré, Akt signalling in health and disease, Cell. Signal. 23 (2011) 1515–1527, https://doi.org/10.1016/j.cellsig.2011.05.004.
[52] L.-Y. Tian, D.J. Smit, N.V. Popova, S. Horn, L.N. Velasquez, S. Huber, M. Jücker, All three AKT Isoforms can Upregulate Oxygen Metabolism and Lactate Production in Human Hepatocellular Carcinoma Cell Lines, Int. J. Mol. Sci. 25 (2024) 2168, https://doi.org/10.3390/ijms25042168.
[53] S. Zhou, L. Liu, H. Li, G. Eilers, Y. Kuang, S. Shi, Z. Yan, X. Li, J.M. Corson, F. Meng, H. Zhou, Q. Sheng, J.A. Fletcher, W.-B. Ou, Multipoint targeting of the PI3K/mTOR pathway in mesothelioma, Br. J. Cancer 110 (2014) 2479–2488, https://doi.org/10.1038/bjc.2014.220.
[54] S.-U. Woo, T. Sangai, A. Akcakanat, H. Chen, C. Wei, F. Meric-Bernstam, Vertical inhibition of the PI3K/Akt/mTOR pathway is synergistic in breast cancer, Oncogenesis 6 (2017) e385, https://doi.org/10.1038/oncsis.2017.86.
[55] R. Rivera-Soto, Y. Yu, D.P. Dittmer, B. Damania, Combined Inhibition of Akt and mTOR is Effective against Non-Hodgkin Lymphomas, Front. Oncol. 11 (2021) 670275, https://doi.org/10.3389/fonc.2021.670275.
[56] A. Szwed, E. Kim, E. Jacinto, Regulation and metabolic functions of mTORC1 and mTORC2, Physiol. Rev. 101 (2021) 1371–1426, https://doi.org/10.1152/physrev.00026.2020.
[57] X. Wan, B. Harkavy, N. Shen, P. Grohar, L.J. Helman, Rapamycin induces feedback activation of Akt signaling through an IGF-1R-dependent mechanism, Oncogene 26 (2007) 1932–1940, https://doi.org/10.1038/sj.onc.1209990.
[58] B.R. Davies, H. Greenwood, P. Dudley, C. Crafter, D.-H. Yu, J. Zhang, J. Li, B. Gao, Q. Ji, J. Maynard, S.-A. Ricketts, D. Cross, S. Cosulich, C.C. Chresta, K. Page, J. Yates, C. Lane, R. Watson, R. Luke, D. Ogilvie, M. Pass, Preclinical pharmacology of AZD5363, an inhibitor of AKT: pharmacodynamics, antitumor activity, and correlation of monotherapy activity with genetic background, Mol. Cancer Ther. 11 (2012) 873–887, https://doi.org/10.1158/1535-7163.MCT-11-0824-T.
[59] S.-B. Kim, R. Dent, S.-A. Im, M. Espié, S. Blau, A.R. Tan, S.J. Isakoff, M. Oliveira, C. Saura, M.J. Wongchenko, A.V. Kapp, W.Y. Chan, S.M. Singel, D.J. Maslyar, J. Baselga, LOTUS investigators, Ipatasertib plus paclitaxel versus placebo plus paclitaxel as first-line therapy for metastatic triple-negative breast cancer (LOTUS): a multicentre, randomised, double-blind, placebo-controlled, phase 2 trial, Lancet Oncol. 18 (2017) 1360–1372, https://doi.org/10.1016/S1470-2045(17)30450-3.
[60] J.S. de Bono, U. De Giorgi, D.N. Rodrigues, C. Massard, S. Bracarda, A. Font, J. A. Arranz Arija, K.C. Shih, G.D. Radavoi, N. Xu, W.Y. Chan, H. Ma, S. Gendreau, R. Riisnaes, P.H. Patel, D.J. Maslyar, V. Jinga, Randomized phase II Study evaluating Akt Blockade with Ipatasertib, in Combination with Abiraterone, in patients with Metastatic Prostate Cancer with and without PTEN loss, Clin. Cancer Res. 25 (2019) 928–936, https://doi.org/10.1158/1078-0432.CCR-18-0981.
[61] R. Dent, M. Oliveira, S.J. Isakoff, S.-A. Im, M. Espié, S. Blau, A.R. Tan, C. Saura, M. J. Wongchenko, N. Xu, D. Bradley, S.-J. Reilly, A. Mani, S.-B. Kim, LOTUS investigators, final results of the double-blind placebo-controlled randomized phase 2 LOTUS trial of first-line ipatasertib plus paclitaxel for inoperable locally advanced/metastatic triple-negative breast cancer, Breast Cancer Res. Treat. 189 (2021) 377–386, https://doi.org/10.1007/s10549-021-06143-5.
[62] N.C. Turner, M. Oliveira, S.J. Howell, F. Dalenc, J. Cortes, H.L.G. Moreno, X. Hu, K. Jhaveri, P. Krivorotko, S. Loibl, S.M. Murillo, M. Okera, Y.H. Park, J. Sohn, M. Toi, E. Tokunaga, S. Yousef, L. Zhukova, E.C. de Bruin, L. Grinsted, G. Schiavon, A. Foxley, H.S. Rugo, Capivasertib in hormone receptor–positive advanced breast cancer, N. Engl. J. Med. 388 (2023) 2058–2070, https://doi.org/10.1056/NEJMoa2214131.
[63] M.B. Nierengarten, FDA approves capivasertib with fulvestrant for breast cancer, Cancer 130 (2024) 835–836, https://doi.org/10.1002/cncr.35238.